Cdc14-dependent dephosphorylation of Inn1 contributes to Inn1–Cyk3 complex formation

Saravanan Palani[1], Franz Meitinger[1], Martin E. Boehm[2], Wolf D. Lehmann[2] and Gislene Pereira[1,*]

[1]Molecular Biology of Centrosomes and Cilia Unit, DKFZ-ZMBH Alliance, German Cancer Research Center (DKFZ), 69120 Heidelberg, Germany
[2]Molecular Structure Analysis, German Cancer Research Center (DKFZ), 69120 Heidelberg, Germany
*Author for correspondence (g.pereira@dkfz.de)

Accepted 27 February 2012
Journal of Cell Science 125, 3091–3096

doi: 10.1242/jcs.106021

Summary

In *Saccharomyces cerevisiae* the Cdc14 phosphatase plays a well-established role in reverting phosphorylation events on substrates of the mitotic cyclin-dependent kinase (M-Cdk1), thereby promoting mitotic exit and downregulation of M-Cdk1 activity. Cdc14 localizes at the site of cell cleavage after M-Cdk1 inactivation, suggesting that Cdc14 may perform a crucial, yet ill-defined, role during cytokinesis. Here, we identified Inn1, as a novel direct substrate of both M-Cdk1 and Cdc14. Cdc14 colocalizes with Inn1 at the cell division site and interacts with the C-terminal proline-rich domain of Inn1 that mediates its binding to the SH3-domain-containing proteins Hof1 and Cyk3. We show that phosphorylation of Inn1 by Cdk1 partially perturbs the interaction of Inn1 with Cyk3 thereby reducing the levels of Cyk3 at the cell division site. We propose that Cdc14 counteracts Cdk1 phosphorylation of Inn1 to facilitate Inn1–Cyk3 complex formation and so promote cytokinesis.

Key words: Cdc14, Cdk1, Cyk3, Hof1, Inn1, Cytokinesis

Introduction

In budding yeast, the successful completion of cytokinesis depends upon the co-ordination of three interdependent processes, the contraction of the actomyosin ring (AMR), ingression of the plasma membrane at the site of cleavage and septum formation. A trimeric complex of Hof1, Inn1 and Cyk3 has been proposed to execute a key function in the coordination between AMR contraction and septum extension (Meitinger et al., 2012; Nishihama et al., 2009; Sanchez-Diaz et al., 2008). The formation of this complex is mediated by the proline-rich C-terminus of Inn1, which interacts with the SH3 domains of Hof1 and Cyk3 (Jendretzki et al., 2009; Nishihama et al., 2009; Sanchez-Diaz et al., 2008). Hof1 possesses an N-terminal F-BAR domain, a potential membrane-binding domain (Aspenström, 2009), whereas Inn1 and Cyk3 have been implicated in activating the transmembrane enzyme Chs2 (Nishihama et al., 2009). Chs2 synthesizes the primary septum (PS), a chitin-rich layer that separates mother from daughter cells (Schmidt et al., 2002). Hof1, Inn1 and Cyk3 are recruited to the AMR prior to AMR contraction (Korinek et al., 2000; Lippincott and Li, 1998; Meitinger et al., 2011; Sanchez-Diaz et al., 2008). However, it is still unclear how this trimeric complex co-ordinates PS ingression with contraction of the contractile AMR and how complex formation is regulated in vivo.

We now show that Inn1 is a target of both M-Cdk1 and Cdc14. In vitro and in vivo analyses reveal that Cdc14 reverts Cdk1 phosphorylation at residues within the C-terminal region of Inn1. Phosphorylation of Inn1 by Cdk1 reduced its ability to bind specifically to Cyk3 in vitro and to maintain Cyk3 at the bud neck in vivo. We therefore propose that Cdc14-dependent Inn1 dephosphorylation promotes the formation of Inn1–Cyk3 complexes at the bud neck as cells exit mitosis.

Results and Discussion

Cdc14 localizes at the site of cell division prior to the onset of cytokinesis

Cdc14 accumulates at the bud neck after mitotic exit (Bembenek et al., 2005). To understand Cdc14 function in cytokinesis, we analyzed the timing of Cdc14 translocation to the bud neck with respect to the timing of septin-ring splitting and AMR contraction. We imaged Cdc14–GFP combined with either Cdc3–mCherry or Myo1–mCherry (monomeric Cherry, red fluorescent protein), as septin and AMR markers, respectively (Fig. 1A–D). Cdc14–GFP accumulated at the bud neck shortly before (1–2 min) the septin ring split at the end of mitosis (Fig. 1A,B, asterisk). Cdc14–GFP recruitment to the Myo1–mCherry ring also preceded the onset of AMR contraction (Fig. 1C,D). However, Cdc14–GFP did not contract with the Myo1–mCherry as it constricted but persisted at the bud neck after AMR contraction (Fig. 1D), suggesting that Cdc14 bud neck association is not dependent upon the AMR. Indeed, Cdc14–GFP bud neck association was Myo1 independent (Fig. 1E; supplementary material Fig. S1A). In contrast, Cdc14–GFP did not localize at the bud neck in *cdc12–6* temperature-sensitive mutants, in which the septin complex disassembles at the restrictive temperature (Fig. 1F) (Haarer and Pringle, 1987). These results indicate that Cdc14 is targeted to the bud neck in a septin-dependent manner prior to the onset of septin splitting and AMR contraction.

Inn1 is a substrate of Cdk1 and Cdc14 in vivo and in vitro

We used the yeast two-hybrid system to screen for putative Cdc14 binding partners that may be involved in cytokinesis. Along with known Cdc14 substrates Bfa1 and Sli15 (Pereira et al., 2002; Pereira and Schiebel, 2003), we identified Inn1 as a strong interactor for Cdc14 (Fig. 1G). Importantly, Inn1 co-localized

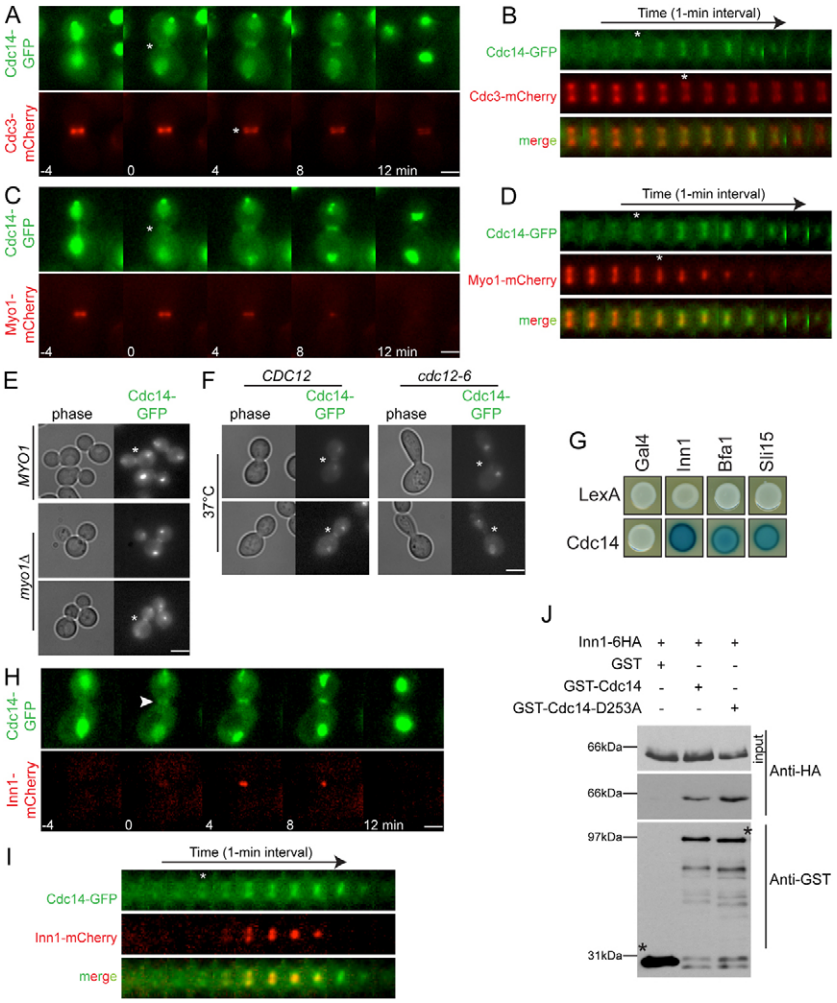

Fig. 1. Timing of Cdc14 bud neck localization. (**A**,**C**) Time-lapse series showing Cdc14–GFP at the bud neck with respect to septin-ring splitting (Cdc3–mCherry) and AMR contraction (Myo1–mCherry). Note that Cdc14–GFP also associates with the nucleolus, nucleus and SPB (Pereira et al., 2002). The asterisks indicate the initial time of Cdc14–GFP bud neck localization, septin splitting and/or onset of AMR contraction. (**B**,**D**) Kymographs of A and C, respectively. (**E**) Cdc14–GFP bud neck localization in *myo1Δ* cells. (**F**) Cdc14–GFP bud neck localization in *cdc12-6* cells. (**G**) Yeast two-hybrid interaction between LexA or LexA–*CDC14* and Gal4 gene fusions, as specified. Development of a blue color indicates interaction. (**H**) Time-lapse images of *CDC14–GFP INN1–mCherry* cells. (**I**) Kymographs of H. (**J**) In vitro binding assay using recombinant GST, GST–Cdc14 or GST–Cdc14-D253A and yeast cell lysates of *INN1–6HA* cells. GST fusion proteins are indicated (asterisks). Phase, phase-contrast images. Scale bars: 3 μm.

with Cdc14 at the bud neck (Fig. 1H,I). Furthermore, Inn1 interacted with bacterially purified glutathione-*S*-transferase–Cdc14 (GST–Cdc14) and even more strongly with the Cdc14 substrate entrapment mutant, GST–Cdc14-D253A (Bloom et al., 2011) (Fig. 1J), further suggesting that Inn1 is a bonafide substrate of Cdc14.

The role played by Cdc14 in dephosphorylating M-Cdk1 targets is well established (Visintin et al., 1998). Indeed, Inn1 co-immunoprecipitated with mitotic B-type cyclin, Clb2, and Cdk1 (encoded by *CDC28*, the sole cyclin-dependent kinase of budding yeast; Fig. 2A). In addition, isolated Clb2–Cdk1 complexes phosphorylated bacterially purified Inn1 in vitro (Fig. 2B). Inn1 is a phosphoprotein that resolves into distinct phosphorylation forms by protein gel electrophoresis (Fig. 2C, bands 1–3; supplementary material Fig. S1B) (Nishihama et al., 2009). To investigate how Cdk1 influences Inn1 phosphorylation in vivo, we used the analog-sensitive *cdk1-as1* mutant, which is selectively inactivated by the ATP analog 1NM-PP1 (Bishop et al., 2000). The inhibition of Cdk1-as1 abolished the appearance of the slowest migrating form of Inn1–6HA (Fig. 2D, lane 6, band 3), whereas the intermediate phosphoforms were merely decreased (Fig. 2D, lane 6, band 2). Therefore, Cdk1 is one of the key protein kinases that contribute to Inn1 phosphorylation in vivo.

To determine whether Cdc14 is able to dephosphorylate Inn1 in vitro, Inn1–6HA was enriched from mitotic yeast cell lysates and treated with bacterially purified maltose binding protein–Cdc14 (MBP–Cdc14). Incubation with this fusion protein reduced the level of the slowest migrating isoform of Inn1–6HA (Fig. 2E, bands 2 and 3), consistent with the reliance upon Cdk1 activity for the appearance of these isoforms in vivo (Fig. 2D). Moreover, in vivo overproduction of active Cdc14, but not of the catalytically inactive Cdc14-C283S mutant protein, similarly decreased phosphorylation of Inn1–6HA (Fig. 2F,G). We conclude that Inn1 is an in vivo and in vitro substrate of both mitotic Cdk1 and Cdc14.

Inn1 is phosphorylated at the proline-rich C-terminus

Inn1 contains eight putative Cdk1 consensus sites (Fig. 3A). Mass spectrometric (MS) analysis established that Cdk1 phosphorylated five sites in the Inn1 C-terminal region of Inn1 in vitro (Fig. 3A; supplementary material Fig. S1C). Although spectra for peptides containing the N-terminal Cdk1 sites were also identified, none of the signatures corresponded to phosphorylated peptides. This suggests that Cdk1 specifically phosphorylates residues in the Inn1 C-terminus of Inn1. We confirmed that serine 364 was phosphorylated in vivo (Fig. 3A; supplementary material Fig. S1B). However, the substitution of serine 364 to a non-phosphorylatable alanine residue (S364A) was not sufficient to impair phosphorylation of Inn1-S364A by Clb2–Cdk1 in vitro (supplementary material Fig. S1D). Instead,

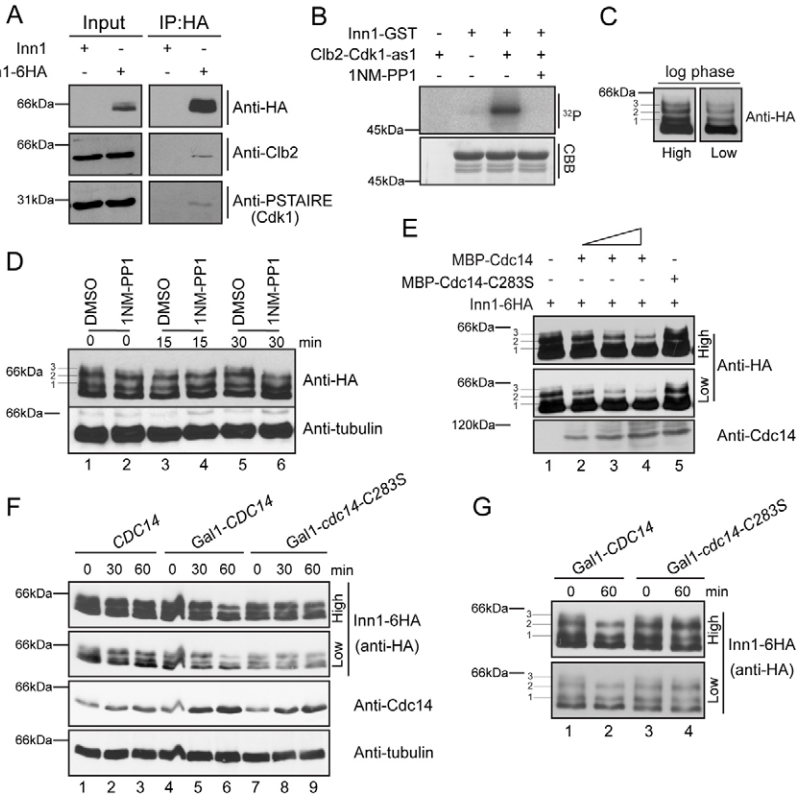

Fig. 2. Inn1 is a direct target of Cdk1 and Cdc14. (**A**) Inn1–6HA was immunoprecipitated from metaphase-arrested cells (nocodazole treatment) and analyzed with the indicated antibodies. (**B**) Autoradiographs showing Inn1 phosphorylation by Clb2–Cdk1-as1 in the absence but not in the presence of the inhibitor 1NM-PP1. CBB, Coomassie Brilliant Blue staining. (**C**) Inn1–6HA phosphorylation patterns in cycling cells. High- and low-exposure immunoblots are shown. (**D**) *INN1–6HA* cells were treated with DMSO (solvent control) or 1NM-PP1 (t=0). Samples were taken at the indicated time points for Inn1–6HA phosphorylation analysis. Tubulin served as loading control. (**E**) In vitro dephosphorylation of Inn1 by Cdc14. Inn1–6HA was immunoprecipitated from yeast cell lysates and incubated for 1 h at 30℃ with buffer (lane 1), increasing amounts of MBP–Cdc14 (0.25, 0.5, 1 µg; lanes 2, 3, 4) or MBP–Cdc14-C283S (1 µg; lane 5). (**F**) α-factor-synchronized (G1 arrest) *INN1–6HA* (lanes 1–3); *INN1–6HA* Gal1–*CDC14* (lanes 4–6) and *INN1–6HA* Gal1–*cdc14-C283S* (lanes 7–9) cells were released in galactose-containing medium in the presence of nocodazole to induce expression from the Gal1 promoter and metaphase arrest, respectively. Tubulin served as loading control. (**G**) The indicated samples from F were analyzed side-by-side for better comparison.

Inn1 phosphorylation in vitro was prevented when all five C-terminal Cdk1 sites were mutated to alanine (Inn1-5A, Fig. 3B). Moreover, the slow migrating forms of Inn1 were decreased in *inn1-5A* cycling or metaphase-arrested cells (Fig. 3C), suggesting that phosphorylation of these residues contributes to the Inn1 phosphorylation pattern generated in vivo. In addition, the C-terminal domain of Inn1 was necessary and sufficient to interact with Cdc14 in the yeast two-hybrid system (supplementary material Fig. S1E), suggesting that Cdk1 and Cdc14 mainly regulate Inn1 function by acting on its C-terminal, proline-rich region.

Dephosphorylation of Inn1 is important for its function in promoting cytokinesis

We employed a genetic approach to investigate how Cdk1 phosphorylation affects Inn1 function in vivo, as previously reported for *inn1* temperature-sensitive mutants (Meitinger et al., 2010). For this, we asked whether either the phospho-inhibitory (Inn1-5A) or phospho-mimetic (Inn1-5E) mutants were able to grow in the absence of *MYO1*, *HOF1* or *CYK3* (Fig. 3D; supplementary material Fig. S2A). Whereas deletion of *HOF1* or *CYK3* did not influence growth of either *inn1-5A* or *inn1-5E* cells (supplementary material Fig. S2A), deletion of *MYO1* impaired growth of *inn1-5E* cells at 23℃ and, even more severely, at 37℃ (Fig. 3D). Thus, constitutive phosphorylation of Inn1 at Cdk1 sites compromises Inn1 function.

Dephosphorylation of Inn1 by Cdc14 stabilizes the interaction between Inn1 and Cyk3

We hypothesized that phosphorylation could influence Inn1 bud neck association. To test this, we compared the recruitment of Inn1 to the bud neck relative to that of the type-V myosin motor Myo2, a marker for cell cycle progression (Fig 3E; supplementary material Fig. S2B). Myo2 associates with the growing bud and accumulates at the bud neck during mitotic exit (Lillie and Brown, 1994). Inn1–GFP translocated to the bud neck concomitantly with Myo2–mCherry (Fig. 3E). The timely localization and levels of Inn1-5A–GFP and Inn1-5E–GFP at the bud neck were comparable to that shown by Inn1–GFP (Fig. 3E,F; supplementary material Fig. S2B,C), suggesting that phosphorylation of Inn1 by Cdk1 does not regulate Inn1 function at the levels of its recruitment to the bud neck.

The C-terminal region of Inn1 was reported to directly bind to Hof1 and Cyk3 (Fig. 4A) (Nishihama et al., 2009). To test whether Cdk1 might influence this interaction between Inn1 and Hof1 and/or Cyk3, we performed in vitro binding assays using a purified C-terminal truncated form of Inn1 (Inn1-C). Immobilized GST and GST–Cyk3 proteins were incubated with purified 6His–Inn1-C, 6His–Inn1-C-5A and 6His–Inn1-C-5E (Fig. 4B). As a negative control, we used an *inn1-C* mutant, in which the four PxxP clusters, including the ones that mediate binding to Hof1 and/or Cyk3 (Fig. 4A), were mutated to alanine (6His–Inn1-C-PxxP). As previously reported (Nishihama et al., 2009), GST–Cyk3 efficiently bound to 6His–Inn1-C but failed to interact with 6His–Inn1-C-PxxP (Fig. 4B, lane 4). Importantly, binding of 6His–Inn1-C-5E to GST–Cyk3 was significantly reduced compared to 6His–Inn1-C and 6His–Inn1-C-5A (Fig. 4B, lanes 1–3). We also observed that Inn1-5E interacted less efficiently with Cyk3 in the yeast two-hybrid system in comparison to Inn1 or Inn1-5A (supplementary material Fig. S2D). Thus, phosphorylation of Inn1 by Cdk1 might decrease the interaction between Inn1 and Cyk3. To confirm this, we performed in vitro binding assays using 6His–Inn1-C

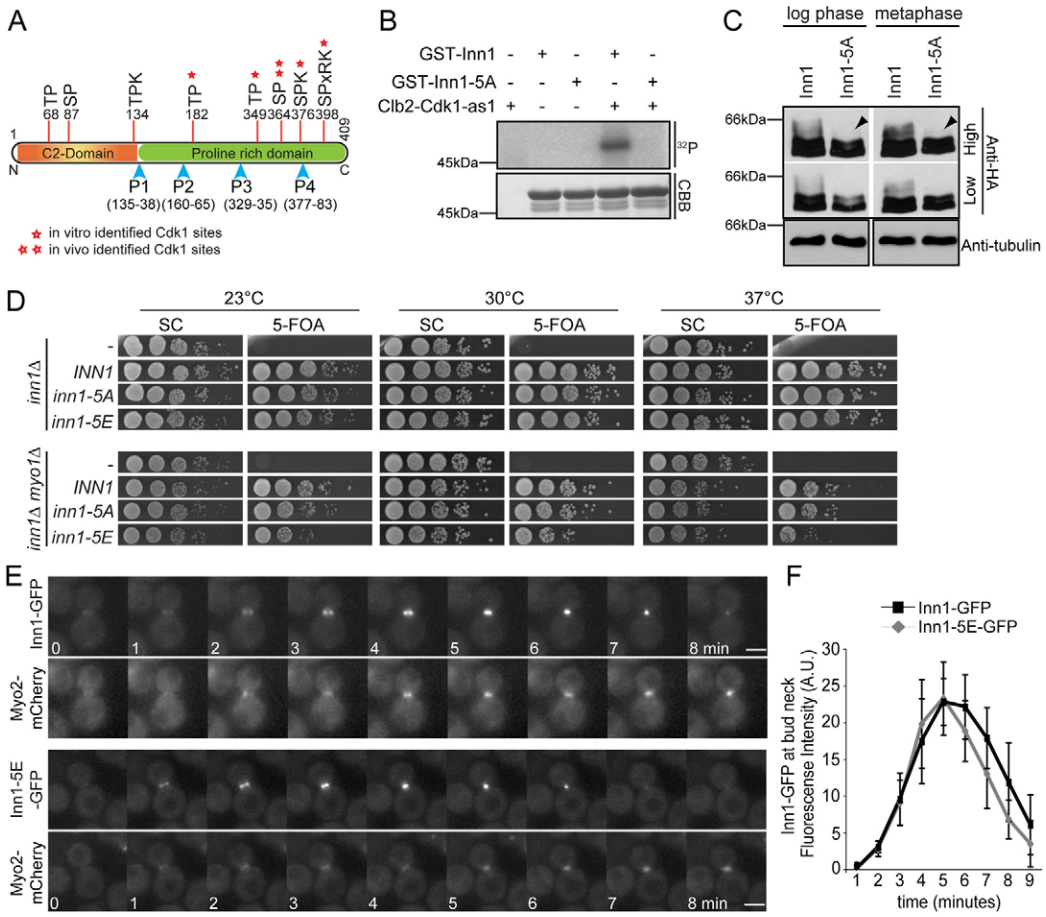

Fig. 3. Clb2–Cdk phosphorylation negatively regulates Inn1 at the bud neck. (**A**) Schematic representation of Inn1 protein domains and Cdk1 consensus sites. P1–P4, PxxP motifs; numbers indicate amino acid positions. (**B**) Autoradiographs showing GST–Inn1 and GST–Inn1-5A phosphorylation by Clb2–Cdk1-as1. CBB, Coomassie Brilliant Blue staining. (**C**) Inn1–6HA and Inn1-5A–6HA phosphorylation pattern in cycling (log phase) and nocodazole-treated (metaphase arrest) cells. Tubulin served as loading control. (**D**) Serial dilutions of *myo1Δ inn1Δ* cells carrying the *URA3*-based plasmid pRS316-*INN1* and *LEU2*-based plasmids pRS315-*INN1*, pRS315-*INN1-5A* or pRS315-*INN1-5E* were spotted on SC-LEU and 5-FOA plates and incubated for 2–3 days at the indicated temperatures. 5-FOA selects against *URA3–INN1*. (**E**) Time-lapse series of *INN1–GFP MYO2–mCherry* and *INN1-5E–GFP MYO2–mCherry* cells. Scale bar: 3 µm. (**F**) Quantification of E ($n=10$ cells per strain). Error bars show the standard errors of the means.

pre-phosphorylated by Clb2–Cdk1-as1 (Fig. 4C). The efficiency of Inn1-C phosphorylation by Clb2–Cdk1-as1 was confirmed by autoradiography using radioactive ATP (data not shown). The interaction between phosphorylated 6His–Inn1-C and GST–Cyk3 was significantly decreased when the kinase was functional when compared to the levels of association in reactions in which the kinase was absent (Fig. 4C, lane 4) or inactive (presence of 1NM-PP1; Fig. 4B, lane 6). Importantly, the interaction between phosphorylated Inn1 and Hof1 was not affected by incubation with the Cdk1 kinase complex (supplementary material Fig. S2E).

If Inn1 phosphorylation were to regulate Inn1–Cyk3 binding in vivo, one would also expect that inhibition of the Inn1–Cyk3 interaction but not the Inn1–Hof1 association would retard the growth of *myo1Δ* cells, as seen in *myo1Δ inn1-5E* mutants (Fig. 3D). Two distinct PxxP clusters mediate the binding of Inn1 to Cyk3 (PxxP cluster 2) and Hof1 (PxxP cluster 4; Fig. 4A). Importantly, the inactivation of the PxxP cluster 2 (*inn1-P2*) but not cluster 4 (*inn1-P4*) impaired growth of *myo1Δ* cells (Fig. 4D). Together, these findings strongly suggest that phosphorylation of Inn1 by Cdk1 perturbs the formation of Inn1–Cyk3 complexes.

Inn1 was previously reported to be required for efficient Cyk3 bud neck localization (Meitinger et al., 2010). We therefore asked whether Inn1-5E was able to recruit Cyk3 to the bud neck. As a control, we followed Cyk3 localization in *inn1-P2* mutants. Interestingly, in both *inn1-5E* and *inn1-P2* cells, the level of Cyk3–GFP recruitment to the bud neck was significantly lower than that seen in either *inn1-5A* or wild-type cells (Fig. 4E,F; supplementary material S2F,G). The decrease of Cyk3 bud neck recruitment was even more pronounced when PxxP cluster 2 and Inn1-5E phosphomimetic mutations were combined (*inn1-P2-5E*; supplementary material Fig. S3A–C). The protein levels of Cyk3–GFP in wild-type, *inn1-5A*, *inn1-5E*, *inn1-P2* and *inn1-P2-5E* cells were similar (supplementary material Fig. S2H,I, Fig. S3D). Therefore, both Inn1 PxxP cluster 2 and phosphoregulation contribute to Cyk3 localization in vivo.

Consequently, we postulated that if the growth defect of the *myo1Δ inn1-5E* mutant was related to an imbalance in the levels of Cyk3 at the bud neck, we should be able to restore growth of

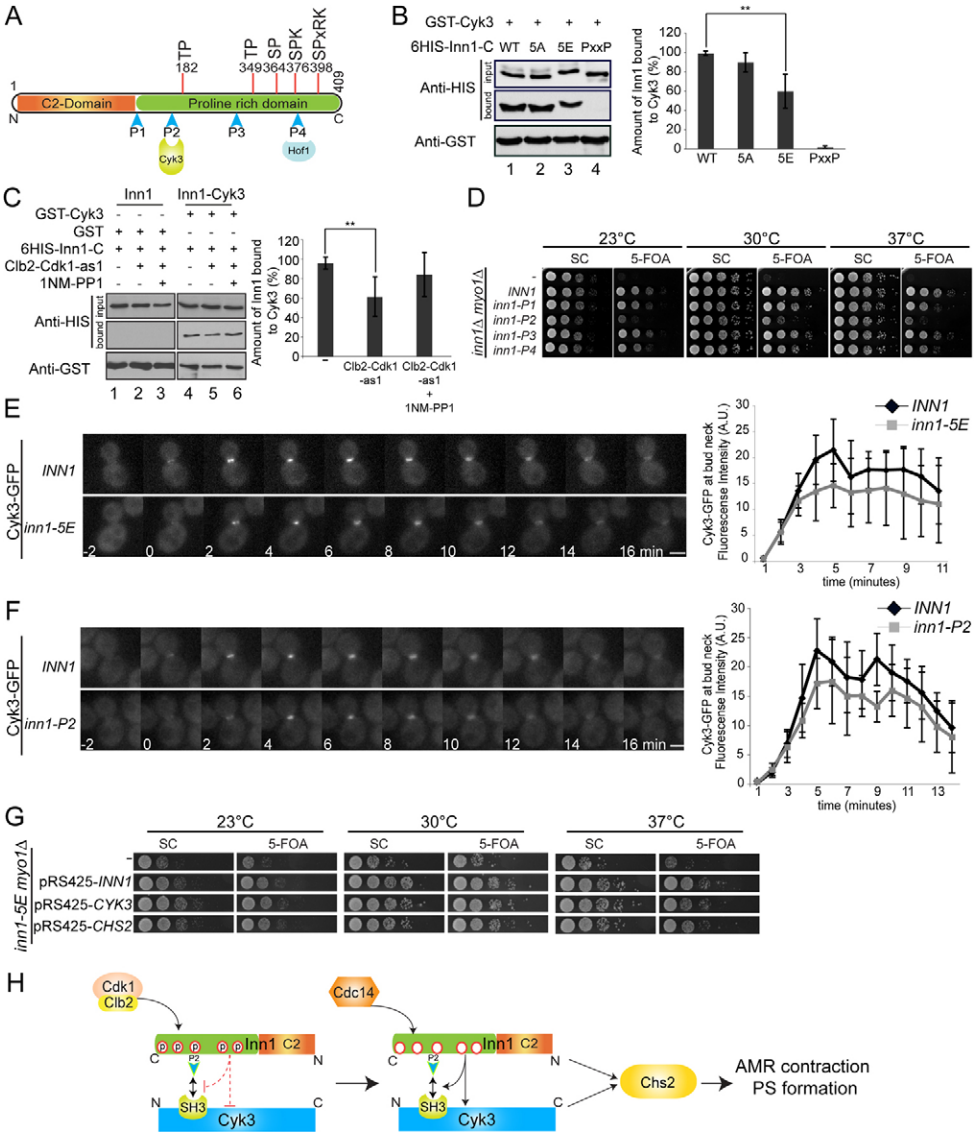

Fig. 4. Phospho-regulation of Inn1 controls Inn1–Cyk3 binding. (**A**) Inn1-PxxP clusters 2 and 4 (P2 and P4) interact with Cyk3 and Hof1, respectively. (**B**) In vitro binding assays using GST-Cyk3 and the indicated Inn1 constructs. The graphs represent the average values of relative binding efficiency of Inn1 to Cyk3 from five independent experiments) Student's *t*-test $^{**}P<0.005$). Input: 10% of the total. (**C**) Same as B, but using in vitro phosphorylated 6His-Inn1-C (as indicated). (**D**) Serial dilutions of *myo1Δ inn1Δ URA3-INN1* cells, carrying the indicated *LEU2*-based constructs, were spotted on SC-LEU and 5-FOA plates and incubated for 2–3 days at the indicated temperatures. (**E**) Time-lapse series and quantification of Cyk3-GFP in INN1 ($n=10$) and inn1-5E ($n=8$) cells. Error bars show the standard error of the means. (**F**) Time-lapse series and quantification of Cyk3-GFP in *INN1* and *inn1-P2* cells ($n=10$ each). Scale bars: 3 µm. (**G**) Growth of *myo1Δ inn1-5E* pRS316-*INN1* cells carrying pRS425 (–) or the indicated constructs. Performed as in (D). (**H**) Phospho-regulation of Inn1 by Cdk1 and Cdc14 regulates its binding to Cyk3 to promote cytokinesis.

inn1-5E cells by overexpressing *CYK3* or a downstream target of Inn1 and Cyk3. Indeed, the overexpression of *CYK3* or the enzyme *CHS2* (a downstream target of Inn1 and Cyk3) (Nishihama et al., 2009), rescued the genetic growth defect of *myo1Δ inn1-5E* cells (Fig. 4G). Given that the localization of neither Chs2–GFP nor Cdc14–GFP was impaired in *inn1-5E* cells in comparison to wild-type *INN1* cells (supplementary material Fig. S3E,F), we concluded that the catalytic activity of Chs2, rather than Cdc14-dependent Chs2 trafficking to the bud neck (Chin et al., 2012), is under control of Inn1 and Cyk3.

We therefore propose that Inn1 becomes phosphorylated by Clb2–Cdk1 at C-terminal residues during mitosis. Our data suggest that this phosphorylation does not regulate the bud neck association of Inn1. Therefore, the lack of bud neck localized Inn1 dictated by high M-Cdk1 activity is most likely to arise from different, additional mechanisms of Cdk1-dependent regulation at the level of repolarization and/or protein transport (Meitinger et al., 2010). With mitotic exit, Cdc14 and Inn1 accumulate at the bud neck. This pool of Cdc14 might counteract Cdk1 phosphorylation of Inn1. Dephosphorylation of Inn1 by Cdc14 may stabilize the association between Inn1 and Cyk3 by either exposing the PxxP cluster 2 or directly potentiate Inn1–Cyk3 association in a PxxP-independent manner (Fig. 4H). Interestingly, Cdc14 was recently shown to dephosphorylate Chs2 at the endoplasmic reticulum to facilitate its translocation to the bud neck (Chin et al., 2012). This observation suggests that Cdc14 promotes Chs2 bud neck accumulation at the same time as it facilitates the formation of the Inn1–Cyk3 complex, which has been proposed to activate Chs2 at the bud neck and so initiate PS formation. In conclusion, the concerted action of Cdc14 upon multiple phospho-substrates, which are most likely not restricted to Chs2 and Inn1, may constitute the underlying mechanism by which cells coordinate cytokinesis with mitotic exit in time and space.

Materials and Methods

Reagents and growth conditions

Yeast strains and plasmids are described in (supplementary material Tables S1, S2). Gene deletions and epitope tagging were performed using PCR-based methods (Janke et al., 2004). Yeast growth conditions and synchronizations were done as described (Caydasi et al., 2010; Meitinger et al., 2010; Sherman, 1991).

Primary antibodies were mouse anti-HIS, anti-PSTAIRE (recognizes Cdk1), anti-tubulin (Tub1), anti-HA (clone 12CA5, Sigma); rabbit anti-GFP, anti-Clb2, guinea-pig anti-Sic1, goat anti-GST (GE Healthcare), and sheep anti-Cdc14 (a gift from E. Schiebel, ZMBH, Germany). Secondary antibodies were coupled to horseradish peroxidase (Jackson ImmunoResearch Laboratories).

Fluorescence microscopy

Time-lapse experiments were performed as described previously (Caydasi and Pereira, 2009). For live-cell imaging of Cdc14–GFP, Inn1–GFP, Chs2–GFP and Cyk3–GFP, five z-stacks of 0.2 µm thickness were taken every minute. Z-stacks were maximum projected using ImageJ software.

Protein purifications, immunoprecipitation and MS analysis

GST and 6His fusion proteins were purified from *Escherichia coli* according to the manufacturer's instructions (GE Healthcare and Qiagen). Clb2–Cdk1-as1 was purified from yeast cells (Ubersax et al., 2003). Immunoprecipitations of Inn1–6HA and Inn1–TAP were performed as described (König et al., 2010). Phosphosite analyses were performed by a combination of immunoprecipitation, one-dimensional PAGE, in-gel digestion using GluC or trypsin, and peptide analysis by nanoUPLC-MS/MS. MS analyses were performed by a nanoUPLC-LTQ-Orbitrap system (nanoAcquity, Waters, Milford, MA or Thermo, Bremen, Germany). Phosphosite annotation was performed automatically using the search engine MASCOT (version 2.2.2) followed by manual control using Xcalibur 2.0.6. For additional information see Seidler et al. (Seidler et al., 2011).

In vitro kinase and in vitro dephosphorylation assays

In vitro kinase and dephosphorylation assays were performed as described (König et al., 2010) using bacterially purified GST- and 6His–Inn1 as substrates. 5 µCi [γ-^{32}P]ATP (0.05 nM) was used per reaction. Radioactivity was detected using a Bas 1800 II imaging system (Fujifilm).

Yeast two-hybrid assay

Indicated genes or gene fragments were cloned into pMM5 and pMM6. The obtained plasmids were transformed in SGY37 and YPH500. Yeast two-hybrid analysis was performed as described previously (Geissler et al., 1996).

In vitro binding assay

GST or GST–Cyk3 (~3 µg) bound to glutathione beads were mixed with ~1 µg 6His–Inn1-C and incubated in binding buffer (PBS, 0.2% NP-40) for 1 h at 4℃. The beads were washed with PBS, 0.5% NP-40 and analyzed by SDS-PAGE and western blotting. Bound Inn1–6HIS was calculated as $(I_{\text{Inn1–6HIS}}–I_{\text{background}})/(I_{\text{GST–Cyk3}}–I_{\text{background}})$, where I is the mean grey value of the protein bands measured using ImageJ (NIH).

Acknowledgements

We thank Elmar Schiebel and Erfei Bi for reagents; Elmar Schiebel, Parthive Patel, Iain Hagan, Fouzia Ahmad and lab members for comments on the manuscript.

Funding

This work was supported by the Marie Curie grant [grant number MEXTCT-042544] to G.P.; S.P. is currently funded by a fellowship from the Landesgraduiertenförderung 'Promotionskolleg, Regulation of Cell Division', University of Heidelberg, Germany. S.P. and F.M. were Marie Curie Fellows. S.P. is a member of Hartmut Hoffmann-Berling International Graduate School (HBIGS).

Supplementary material available online at
http://jcs.biologists.org/lookup/suppl/doi:10.1242/jcs.106021/-/DC1

References

Aspenström, P. (2009). Roles of F-BAR/PCH proteins in the regulation of membrane dynamics and actin reorganization. *Int. Rev. Cell Mol. Biol.* **272**, 1-31.

Bembenek, J., Kang, J., Kurischko, C., Li, B., Raab, J. R., Belanger, K. D., Luca, F. C. and Yu, H. (2005). Crm1-mediated nuclear export of Cdc14 is required for the completion of cytokinesis in budding yeast. *Cell Cycle* **4**, 961-971.

Bishop, A. C., Ubersax, J. A., Petsch, D. T., Matheos, D. P., Gray, N. S., Blethrow, J., Shimizu, E., Tsien, J. Z., Schultz, P. G., Rose, M. D. et al. (2000). A chemical switch for inhibitor-sensitive alleles of any protein kinase. *Nature* **407**, 395-401.

Bloom, J., Cristea, I. M., Procko, A. L., Lubkov, V., Chait, B. T., Snyder, M. and Cross, F. R. (2011). Global analysis of Cdc14 phosphatase reveals diverse roles in mitotic processes. *J. Biol. Chem.* **286**, 5434-5445.

Caydasi, A. K. and Pereira, G. (2009). Spindle alignment regulates the dynamic association of checkpoint proteins with yeast spindle pole bodies. *Dev. Cell* **16**, 146-156.

Caydasi, A. K., Kurtulmus, B., Orrico, M. I., Hofmann, A., Ibrahim, B. and Pereira, G. (2010). Elm1 kinase activates the spindle position checkpoint kinase Kin4. *J. Cell Biol.* **190**, 975-989.

Chin, C. F., Bennett, A. M., Ma, W. K., Hall, M. C. and Yeong, F. M. (2012). Dependence of Chs2 ER export on dephosphorylation by cytoplasmic Cdc14 ensures that septum formation follows mitosis. *Mol. Biol. Cell* **23**, 45-58.

Geissler, S., Pereira, G., Spang, A., Knop, M., Soues, S., Kilmartin, J. and Schiebel, E. (1996). The spindle pole body component Spc98p interacts with the gamma-tubulin-like Tub4p of *Saccharomyces cerevisiae* at the sites of microtubule attachment. *Embo J* **15**, 3899-3911.

Haarer, B. K. and Pringle, J. R. (1987). Immunofluorescence localization of the Saccharomyces cerevisiae CDC12 gene product to the vicinity of the 10-nm filaments in the mother-bud neck. *Mol. Cell. Biol.* **7**, 3678-3687.

Janke, C., Magiera, M. M., Rathfelder, N., Taxis, C., Reber, S., Maekawa, H., Moreno-Borchart, A., Doenges, G., Schwob, E., Schiebel, E. et al. (2004). A versatile toolbox for PCR-based tagging of yeast genes: new fluorescent proteins, more markers and promoter substitution cassettes. *Yeast* **21**, 947-962.

Jendretzki, A., Ciklic, I., Rodicio, R., Schmitz, H. P. and Heinisch, J. J. (2009). Cyk3 acts in actomyosin ring independent cytokinesis by recruiting Inn1 to the yeast bud neck. *Mol. Genet. Genomics* **282**, 437-451.

König, C., Maekawa, H. and Schiebel, E. (2010). Mutual regulation of cyclin-dependent kinase and the mitotic exit network. *J. Cell Biol.* **188**, 351-368.

Korinek, W. S., Bi, E., Epp, J. A., Wang, L., Ho, J. and Chant, J. (2000). Cyk3, a novel SH3-domain protein, affects cytokinesis in yeast. *Curr. Biol.* **10**, 947-S4.

Lillie, S. H. and Brown, S. S. (1994). Immunofluorescence localization of the unconventional myosin, Myo2p, and the putative kinesin-related protein, Smy1p, to the same regions of polarized growth in Saccharomyces cerevisiae. *J. Cell Biol.* **125**, 825-842.

Lippincott, J. and Li, R. (1998). Dual function of Cyk2, a cdc15/PSTPIP family protein, in regulating actomyosin ring dynamics and septin distribution. *J. Cell Biol.* **143**, 1947-1960.

Meitinger, F., Petrova, B., Lombardi, I. M., Bertazzi, D. T., Hub, B., Zentgraf, H. and Pereira, G. (2010). Targeted localization of Inn1, Cyk3 and Chs2 by the mitotic-exit network regulates cytokinesis in budding yeast. *J. Cell Sci.* **123**, 1851-1861.

Meitinger, F., Boehm, M. E., Hofmann, A., Hub, B., Zentgraf, H., Lehmann, W. D. and Pereira, G. (2011). Phosphorylation-dependent regulation of the F-BAR protein Hof1 during cytokinesis. *Genes Dev.* **25**, 875-888.

Meitinger, F., Palani, S. and Pereira, G. (2012). The power of MEN in cytokinesis. *Cell Cycle* **11**, 219-228.

Nishihama, R., Schreiter, J. H., Onishi, M., Vallen, E. A., Hanna, J., Moravcevic, K., Lippincott, M. F., Han, H., Lemmon, M. A., Pringle, J. R. et al. (2009). Role of Inn1 and its interactions with Hof1 and Cyk3 in promoting cleavage furrow and septum formation in S. cerevisiae. *J. Cell Biol.* **185**, 995-1012.

Pereira, G. and Schiebel, E. (2003). Separase regulates INCENP-Aurora B anaphase spindle function through Cdc14. *Science* **302**, 2120-2124.

Pereira, G., Manson, C., Grindlay, J. and Schiebel, E. (2002). Regulation of the Bfa1p-Bub2p complex at spindle pole bodies by the cell cycle phosphatase Cdc14p. *J. Cell Biol.* **157**, 367-379.

Sanchez-Diaz, A., Marchesi, V., Murray, S., Jones, R., Pereira, G., Edmondson, R., Allen, T. and Labib, K. (2008). Inn1 couples contraction of the actomyosin ring to membrane ingression during cytokinesis in budding yeast. *Nat. Cell Biol.* **10**, 395-406.

Schmidt, M., Bowers, B., Varma, A., Roh, D. H. and Cabib, E. (2002). In budding yeast, contraction of the actomyosin ring and formation of the primary septum at cytokinesis depend on each other. *J. Cell Sci.* **115**, 293-302.

Seidler, J., Zinn, N., Haaf, E., Boehm, M. E., Winter, D., Schlosser, A. and Lehmann, W. D. (2011). Metal ion-mobilizing additives for comprehensive detection of femtomole amounts of phosphopeptides by reversed phase LC-MS. *Amino Acids* **41**, 311-320.

Sherman, F. (1991). Getting started with yeast. *Methods Enzymol.* **194**, 3-21.

Ubersax, J. A., Woodbury, E. L., Quang, P. N., Paraz, M., Blethrow, J. D., Shah, K., Shokat, K. M. and Morgan, D. O. (2003). Targets of the cyclin-dependent kinase Cdk1. *Nature* **425**, 859-864.

Visintin, R., Craig, K., Hwang, E. S., Prinz, S., Tyers, M. and Amon, A. (1998). The phosphatase Cdc14 triggers mitotic exit by reversal of Cdk-dependent phosphorylation. *Mol. Cell* **2**, 709-718.